Chain Stiffness of Copolycarbonates Containing a Spiro Linkage

R. Wimberger-Friedl,* M. G. T. Hut, and H. F. M. Schoo

Philips Research Laboratories, Prof. Holstlaan 4, 5656 AA Eindhoven, The Netherlands

Received August 22, 1995; Revised Manuscript Received March 21, 1996[⊗]

ABSTRACT: Physical properties relating to chain stiffness are determined for a series of copolycarbonates of Bisphenol A and 1,1′-spiro[bis(3,3′-dimethyl-6-hydroxyindan)] (SBI) of varying composition. The entanglement molecular weight, M_e, is derived from the rubbery plateau modulus. The recoverable compliance, J_e^0, is determined from the dynamic moduli as well as from steady shear creep and recovery experiments. It is found that all properties change in a nonlinear fashion with SBI content. For small SBI content the entanglement density is hardly affected, whereas T_g and J_e^0 increase strongly. With further increase in SBI content the effect on T_g is less pronounced. M_e, however, starts increasing progressively to about 10 times that of pure Bisphenol A polycarbonate. The functional dependence of M_e on composition is not predicted correctly from group contributions.

1. Introduction

Bisphenol A polycarbonate (BPA-PC) is known to have a highly flexible chain. Molecular mechanics simulations show that the energy barriers for rotation about the C−O bonds of the carbonate group, as well as for rotation about the C−C bonds between the phenyl and the isopropylidene unit, are rather low.[1,2] Consequently, the molecular weight between entanglements M_e is only around 2000,[3] which corresponds to eight repeating units. Many unsubstituted, aromatic, so-called main-chain polymers, like polyarylates, exhibit high flexibility, in contrast to polymers with bulky side groups, such as polystyrene (PS) or poly(methyl methacrylate) (PMMA). The latter have about a decade higher M_e due to the steric hindrance from the side group, leading to a high persistence length. In the case of PC it was shown that a substitution at the ortho position of the phenyl ring, as in tetramethylpolycarbonate (TMPC), leads to an increase of M_e by about a factor of 2.[3] This is also reflected in a higher glass transition temperature, T_g.

A much more drastic way of increasing the rigidity of the PC chain is to lock in the isopropylidene linkage via a so-called spiro coupling between the phenyl rings, as is the case in the 1,1′-spiro[3,3′-dimethyl-6-hydroxyindan]polycarbonate (SBI−PC). In Figure 1 the chemical configuration is sketched for SBI−PC together with that of conventional BPA-PC. In this way the chemical character and the polarity of the chain should hardly be affected, while the stiffness is increased. This enables the effect of chain stiffness to be studied with minimum additional contributions from interchain interactions. Since the reactivities of SBI and BPA monomers are comparable, random copolymers can be synthesized at any composition.

The entanglement molecular weight is an important factor for both the processibility and the mechanical properties of a polymer.[4] If the weight-average molecular weight M_w is close to the critical molecular weight for entanglement coupling M_c ($\approx 2M_e$[5]), the polymer loses its strength. On the other hand, the viscosity increases by the 3.4th power of M_w from M_c onward. So for good processibility it is desirable to keep M_w as low as possible, especially for high T_g polymers. The dimensional stability of polymer products is also affected by the molecular properties. Flow-induced stresses lead to frozen-in molecular orientation in molded products.[6] This orientation embodies a certain degree of frozen-in residual strain which is a potential threat to the dimensional stability at elevated temperatures. The frozen-in strain is coupled to the flow-induced stresses via the recoverable compliance, J_e^0. This property scales inverse to the entanglement density and consequently with chain stiffness.

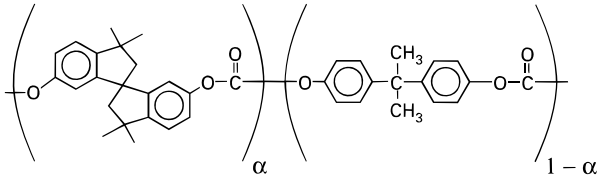

Figure 1. Schematic chemical structure of BPA−SBI copolycarbonates.

The aim of the present investigation was to determine the effect of molecular modification on the chain stiffness in a homologous series of copolycarbonates for the purpose of understanding the principal effects and their consequences for the rheological and mechanical properties of these materials.

2. Experimental Section

Material Synthesis. The SBI−PC copolymers were synthesized in our laboratory. The SBI monomer was prepared as described by Stueben.[7] The polymerization was carried out at the interface of NaOH/water with a pH of 10−11 and CH_2Cl_2 at a temperature of 30 °C by passing through phosgene. The organic phase was separated and washed with acidic water and pure water. The polymer was precipitated twice with methanol and dried for several days in a vacuum oven at 120 °C. Films were cast from dichloromethane solutions and used after careful drying for compression molding. Copolymers of compositions of 27, 46, 65, and 86 mol % SBI were prepared. The copolymers are designated by the SBI content in mole percent. The Bisphenol A homopolymer was Makrolon CD 2000/00000 from Bayer AG, Germany. This is an optical grade free of additives.

Material Characterization. The composition of the copolymers was determined by NMR. The molecular weight distribution was determined after compression molding by gel permeation chromatography (GPC) in $CHCl_3$ relative to PS standards (Polymer Laboratories, U.K.). The results of the GPC measurements are summarized in Table 1. The widths of the distributions are not identical but typical for a conden-

[⊗] Abstract published in *Advance ACS Abstracts,* June 15, 1996.

Table 1. Molecular Weight Characteristics[a]

material	$\bar{M}_w$ [$\times 10^3$]	$\bar{M}_n$ [$\times 10^3$]	dispersion
CD 2000	33	13	2.6
spiro27	62	20	3.1
spiro46	142	35	4.1
spiro65	113	30	3.7
spiro86	136	24	5.6

[a] Note: The values are uncorrected with reference to PS standards.

sation polymerization. The T_g's were determined by differential scanning calorimetry (DSC 7, Perkin Elmer) with a heating rate of 10 K/min (second heating scan) and by dynamic mechanical analysis (DMTA MkIII, Rheometric Scientific, U.K.) at a frequency of 1 Hz and a heating rate of 2 K/min. The densities of the copolymers were determined in a gradient column (Davenport, U.K.) with a K_2CO_3 solution at room temperature.

The dynamic moduli were determined by oscillatory shear experiments in a plate−plate arrangement (Rheometrics RDS-II) at the Eindhoven University of Technology. First a strain sweep was carried out to determine the linear range. This was followed by a number of isothermal frequency sweeps at different temperatures, starting at the highest frequency. A correction of 2 μm/K to the gap width was made for the expansion of the apparatus. Excess material at the rim was removed by hand. The last measurement was chosen identical to the first one in order to check degradation effects in the sample, since the same sample was used for different temperatures.

The steady shear experiments were carried out at DSM Research on a noncommercial rheogoniometer with a cone−plate and a plate−plate arrangement. A torque was applied to the upper plate by means of a load connected via a filament to a wheel on the axis supported by an air bearing. The torsion was detected optically with a resolution of 1.26×10^{-4} rad. Creep experiments followed by recovery were carried out at different stress levels, from 0.9 to 19 kPa.

3. Results and Discussion

Entanglement Molecular Weight, M_e. From ideal rubber elasticity it is known that the molecular weight between entanglements M_e is inversely proportional to the rubbery plateau modulus:[3,5,8]

$$M_e = \rho RT/G_N^0 \tag{1}$$

where ρ represents the density, R the universal gas constant, and T the absolute temperature. Since the rubbery plateau is not really horizontal for most thermoplastic polymers, G_N^0 was defined as the dynamic modulus at the frequency of minimum damping:[3]

$$G_N^0 = [G'(\omega)]_{\tan\delta \to \min} \tag{2}$$

G_N^0 was determined from the master curves of the dynamic moduli which were obtained by horizontal shifting according to the time−temperature superposition principle. The density was extrapolated from room temperature by correcting for thermal expansion with thermal expansion coefficients of 2×10^{-4} K^{-1} below the glass transition T_g and 6×10^{-4} K^{-1} above T_g. In some cases a small vertical shift was allowed in addition to the ideal vertical shift factor, b_T, in order to obtain good superposition of the dynamic moduli curves:

$$b_T = \rho T/\rho_0 T_0 \tag{3}$$

Parts a−c of Figure 2 show the results for CD 2000. In Figure 2a the loss angle is plotted for the various measurement temperatures together with the master curve. Good superposition is obtained. The loss angle

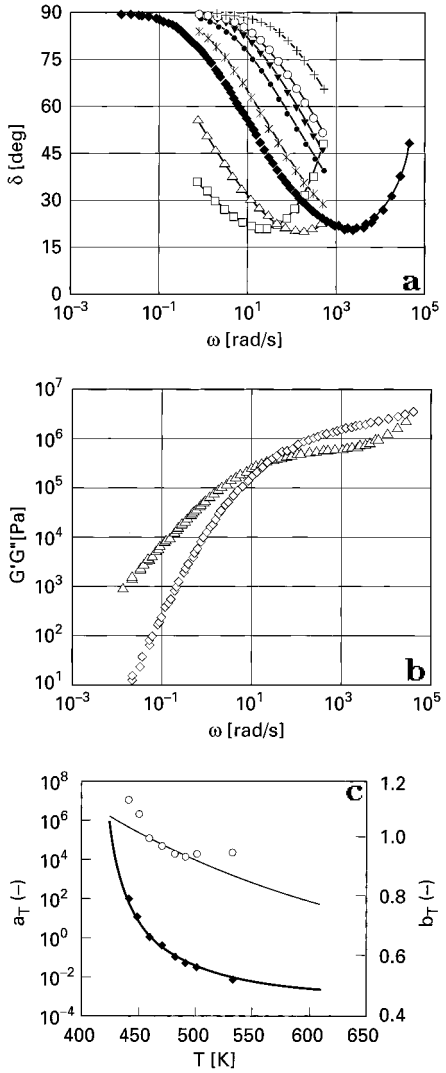

Figure 2. (a) Loss angle, δ, of CD 2000 for different temperatures and master curve at 462 K obtained by horizontal shifting: (+) 533, (○) 502, (▼) 493, (●) 484, (∗) 472, (◆) 462, (△) 452, (□) 443 K. (b) Master curve of the dynamic moduli of CD 2000 at a reference temperature of 462 K: (△) G'', (◇) G'. (c) Horizontal and vertical shift factors appertaining to the master curves in parts a and b. Solid lines are the result of fits with eqs 3 and 4, respectively. (◆) a_T, (○) b_T.

ranges from 90° in the terminal zone to a minimum of about 20° in the rubbery plateau region. This clearly shows that the behavior of the rubbery plateau is not ideally elastic. The horizontal shift factors, a_T, are shown in Figure 2c. The temperature dependence of a_T obeys the WLF equation:[5]

$$\log a_T = \frac{-C_1(T - T_0)}{C_2 + T - T_0} \tag{4}$$

The result of the WLF fit is indicated as a solid line in Figure 2c. The dynamic moduli were shifted by the same factors. Additionally, a vertical shift of b_T is applied. The resulting master curves are depicted in Figure 2b and the vertical shift factors in Figure 2c. The solid line in Figure 2c is the ideal shift according to eq 3.

The results for the copolymers spiro27, -46, -65, and -86 are presented as loss angle and dynamic moduli master curves in Figures 3−6, respectively. In all cases the minimum loss angle is well covered. The limiting slopes of the moduli at low frequencies, which will be used later on to determine the recoverable compliance,

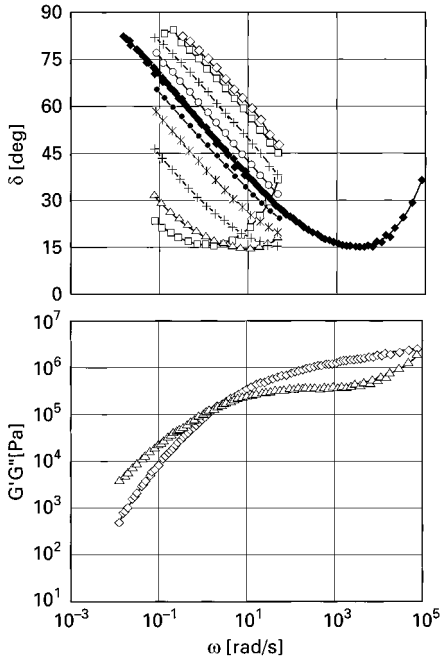

Figure 3. Loss angle and dynamic moduli versus frequency for spiro27. Measurement temperatures: 622, 607, 587, 568, 548, 533, 518, 504, 489, and 481 K; master curve at 548 K.

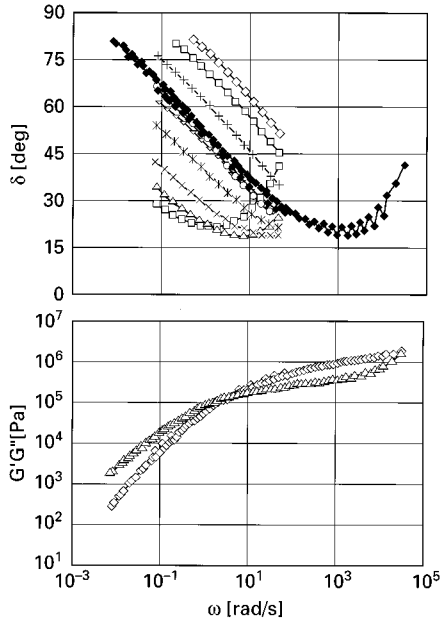

Figure 4. Loss angle and dynamic moduli versus frequency for spiro46. Measurement temperatures: 469, 626, 602, 577, 563, 544, 529, 514, 507, and 502 K; master curve at 563 K.

are not reached completely. The resulting plateau moduli of the copolymers are shown in Figure 7 as a function of the SBI content (in vol %) together with the T_g's obtained from DSC and DMTA measurements, respectively. The corresponding numerical values are listed in Table 2. As can be seen in Figure 7, there is a consistent correlation of G_N^0 and T_g with SBI content. G_N^0 decreases by about a factor of 10 by replacing the BPA by the SBI monomer. The lines drawn in Figure 7 are meant merely to guide the eye and do not represent calculated relationships. It is clear that the correlations are nonlinear. The effect of the spiro linkage on G_N^0 is the weakest at low concentrations of SBI. T_g, on the contrary, is most strongly affected at low SBI content. The T_g of the copolymers cannot be fitted by the Fox relation,[9] which would yield a positive

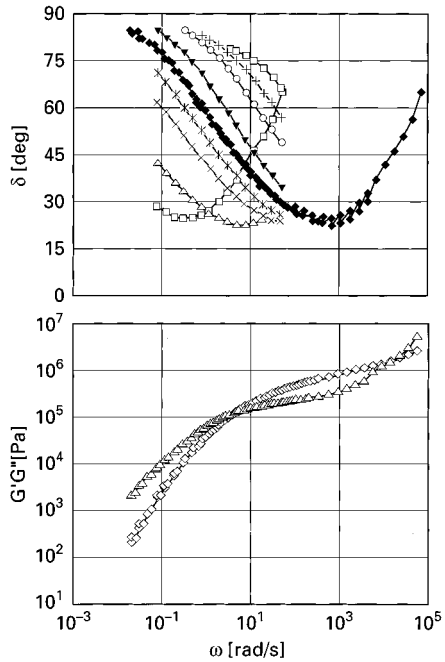

Figure 5. Loss angle and dynamic moduli versus frequency for spiro65. Measurement temperatures: 658, 631, 612, 591, 573, 551, 538, 523, and 513 K; master curve at 573 K.

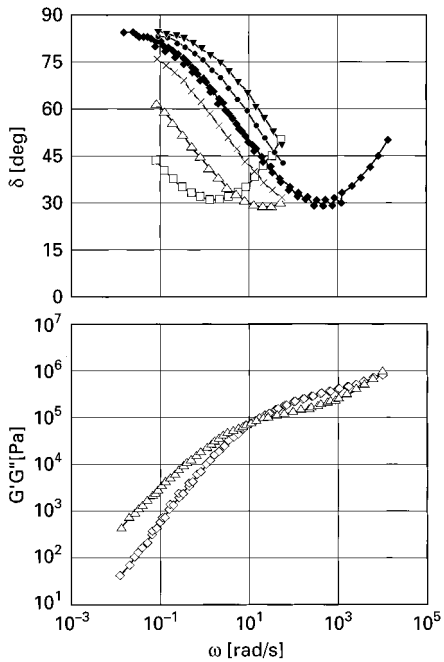

Figure 6. Loss angle and dynamic moduli versus frequency for spiro86. Measurement temperatures: 598, 584, 569, 555, 536, and 521 K; master curve at 569 K.

curvature. Couchman[10] gave a more general relation for the T_g of random solutions, viz.:

$$\ln T_g = \frac{X_1 \Delta c_{p,1} \ln T_{g,1} + X_2 \Delta c_{p,2} \ln T_{g,2}}{X_1 \Delta c_{p,1} + X_2 \Delta c_{p,2}} \qquad (5)$$

where X is the volume fraction and Δc_p the change in heat capacity at the glass transition. The T_g's as shown in Figure 7 can be fitted perfectly by the equation of Couchman, however, only when the change in heat capacity at T_g for the SBI component is taken to be twice that of the BPA component ($\Delta c_{p,2} = 2\Delta c_{p,1}$), which is very unrealistic.

Functional forms for the variation of G_N^0 with composition have been proposed in the literature, for

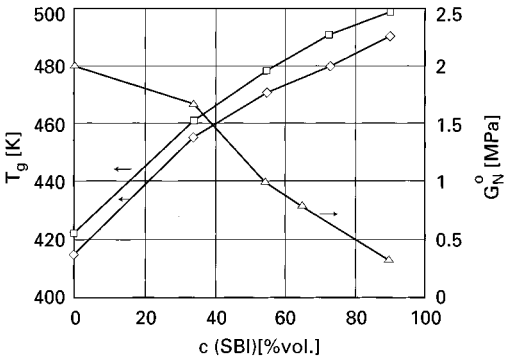

Figure 7. Glass transition temperature (□, DMTA; ◇, DSC) and plateau modulus (△) of copolycarbonates vs SBI content in % (v/v) at a reference temperature of 573 K.

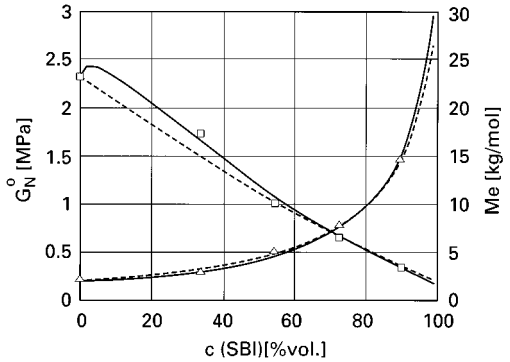

Figure 8. Plateau modulus (□) and entanglement molecular weight (△) of copolycarbonates vs SBI content in % (v/v). Solid line fit by the Tsenoglou model (eq 6); broken line fit by the Wu model (eq 7).

Table 2. T_g, G_N^0, and M_e of SBI Copolycarbonates

material	T_g(DSC) [K]	T_g(DMTA) [K]	G_N^0 [MPa]	T_{ref} [K]	M_e
CD 2000	415	422	2.00	462	2180
spiro27	456	462	4.68	548	2950
spiro46	471	478	1.00	563	4960
spiro65	480	491	0.64	573	7730
spiro86	490	499	0.33	569	14750

instance, by Wu[11] and Tsenoglou,[12] which are similar in the sense that in both models the contributions scale with the square of the volume fractions and the mixed term is adjustable. In Tsenoglou's model:

$$\sqrt{G} = v_1\sqrt{G_1}\left[1 + \epsilon\frac{v_2\sqrt{G_2}}{v_1\sqrt{G_1}}\right]^{\pm 1/2} + v_2\sqrt{G_2}\left[1 + \epsilon\frac{v_1\sqrt{G_1}}{v_2\sqrt{G_2}}\right]^{\pm 1/2} \quad (6)$$

in the case of no specific interactions $\epsilon = 0$. The exponent can either be positive or negative for favored or unfavored contacts between dissimilar components. In Wu's model:[11]

$$G = v_1^2 G_1 + v_2^2 G_2 + 2v_1 v_2 RT\frac{\sqrt{\rho_1\rho_2}}{M_{e,12}} \quad (7)$$

$M_{e,12}$ is a measure for the interaction of dissimilar species, the molecular weight between "hetero" entanglements. In Figure 8 the results are shown of a fit of the measured plateau moduli (after translation to the same reference temperature of 573 K) and M_e by both models. As can be seen, the fit of M_e is very good for both models, although a little better for the Tsenoglou model. This is more clear in the fit of G_N^0. Wu's model does not give a good fit at lower SBI content. The local maximum in Tsenoglou's model cannot be verified with the employed copolymer compositions, unfortunately. In both cases the G_N^0 of pure SBI−PC was taken as 144 kPa. The fit with eq 6 was achieved with a positive exponent and $\epsilon = 0.35$, indicating a favorable interaction between dissimilar components. The fit with Wu's model in Figure 8 was obtained by taking $M_{e,12} = 4700$. In terms of Wu's model this means that the entanglement probability of dissimilar components is higher than that in the unperturbed case. This is different from examples reported in the literature for miscible blends[11] and statistical copolymers of immiscible components.[13] Also the logarithmic blending law, as found by Wu and Beckerbauer[18] for copolymers, is not obeyed by the SBI copolycarbonates.

For both T_g and M_e, there is also an influence coming from the dispersion which is not considered here explicitly, since the various copolymers do not differ very much in that respect. Although M_e is, in principle, only a function of chain stiffness, its determination from the dynamic moduli introduces influences coming from M_w and the dispersion. The former determines the distance from the glass transition relaxation and consequently the degree of overlap of the terminal and glass relaxations, which affects the position of the minimum damping. The dispersion affects the result via the contribution of chains with a molecular weight less than M_c. This dilution leads to apparently higher M_e's. It was shown by Schausberger et al.[14] that G_N^0 scales with the square of the volume fraction of chains with $M \geq M_c$.

Recoverable Compliance, J_e^0. Like the plateau modulus, the recoverable compliance is a rheological property which, in principle, does not scale with molecular weight. Strictly speaking, this holds only for monodisperse polymers, since polydispersity affects J_e^0. The recoverable compliance is a measure of the strain in the physical network of a polymer melt per unit stress:

$$J_e^0 = \lim_{t\to\infty}\frac{\gamma_r}{\sigma_0} \quad (8)$$

where γ_r is the recoverable strain. There are two direct ways of determining γ_r, viz., from creep and from recovery. In a creep experiment a step stress is applied. The total strain is the sum of a recoverable, an elastic, and a plastic contribution:

$$\gamma(t) = \sigma_0\left(J_e(t) + \frac{t}{\eta_0}\right) \quad (9)$$

where η_0 is the zero-shear viscosity. After some time a steady state is reached, where the recoverable compliance becomes constant, namely, equal to J_e^0. If, at a certain point in time, t', the load is removed, the response will be the same as that of applying a negative stress of equal magnitude, in accordance with the Boltzmann superposition principle. The strain can then be written as:

$$\gamma(t) = \sigma_0\left(J_e^0 + \frac{t'}{\eta_0} - J_e(t - t')\right) \quad (10)$$

Again, $J_e(t)$ will eventually become equal to J_e^0, so that only the constant viscous contribution will remain.

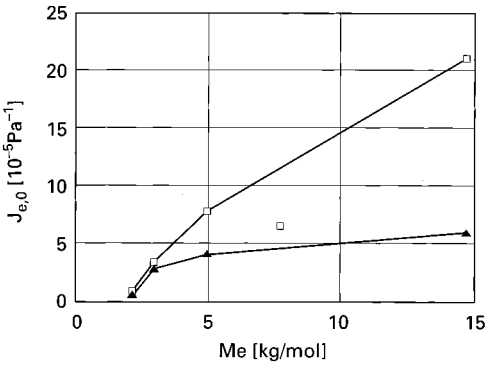

Figure 9. Recoverable shear compliance versus entanglement molecular weight of copolycarbonates: (▲) from recovery; (□) from dynamic moduli.

Table 3. Recoverable Compliance

material	J_e^0(dynamic) [10^{-5} Pa^{-1}]	T_{ref} [K]	J_e^0(recovery) [10^{-5} Pa^{-1}]	T_{meas} [K]
CD 2000	0.6	462	0.5	438, 448
spiro27	3.4	548	2.9	493
spir46	7.7	563	4.1	508
spiro65	6.4	573		
spiro86	20.9	569	5.8	515, 526

Both experiments have their practical difficulties. In the case of creep, any slack in the setup or overshoots in the load will be reflected directly in the value of J_e^0. In the case of recovery, the stress must be exactly zero. Air bearings can have a residual momentum. In both experiments the time scale is critical, as one has to be sure that the steady state has been reached. In both, control of the normal force is also crucial for the reliability of the result, especially in a cone−plate arrangement.

An alternative way of determining J_e^0 is from dynamic moduli at the zero-frequency limit:[5]

$$J_e^0 = \frac{\psi_{1,0}}{2\eta_0^2} = \lim_{\omega \to 0}\left(\frac{G'}{(G'')^2}\right) \tag{11}$$

where $\psi_{1,0}$ is the first normal stress coefficient. This method of determination only requires the limiting slopes of 1 and 2 for G'' and G' on a double-logarithmic plot to be achieved. The experimental results for the copolycarbonates are summarized in Table 3. Only the steady shear results from recovery were used, since the results from creep proved unreliable owing to startup transients. As can be seen from Table 3, J_e^0 increases by more than 1 decade. The values from the steady shear experiments are consistently lower than those from the dynamic experiments. This is obviously due to the fact that the limiting recovery was not reached in the experiments. But even the values from the dynamic experiments can be considered underestimates of the real J_e^0, since the limiting slopes were not reached completely for the copolymers. Instead, the values at the lowest frequency of the master curves were used for the calculations. The value for spiro65 does not fit very well. This is partially due to some scatter of the storage modulus at low frequencies, as can be seen in Figure 5. In Figure 9 the experimental J_e^0 is plotted versus the entanglement molecular weight for all copolycarbonates. In the case when only M_e changes, J_e^0 should change in proportion to it. Both properties scale inversely with the plateau modulus. In terms of dynamic moduli this is merely a vertical shift of the curves. As can be seen in Figure 9, the initial slope, i.e., from the homopolymer to spiro27, is very high. This means that J_e^0 is very sensitive to small SBI concentrations, as was also observed for T_g. (Compare Figure 7). At higher concentrations the average slope is on the order of unity, as could have been expected. An explanation for this strong effect on J_e^0 cannot be given at the moment. From the shape of the dynamic moduli curves one can see that the transition from the rubbery plateau to the terminal regime is more gradual in the case of copolymers. This effect may be interpreted by differences in lifetimes of entanglements depending on the local chemical compositions, leading to a broadening of the spectrum by statistical variations in chemical composition. Another influence may come again from differences in polydispersity. For a polymer the product of G_N^0 and J_e^0 increases strongly with dispersion. Part of the large difference between the J_e^0 of CD2000 and spiro27 could be explained by such an effect.

Characteristic Ratio, C_∞. The prime measure for chain stiffness is the so-called characteristic ratio, C_∞:[15]

$$C_\infty = \langle r_0^2 \rangle / nl^2 \tag{12}$$

This is the ratio of the mean end-to-end distance of the real chain to that of an unperturbed chain of equal contour length, nl, where n is the number of statistical segments and l is their length. Wu gave a relation between the characteristic ratio and the entanglement molecular weight based on his binary hooking model for entanglements:[3]

$$N_v = 3C_\infty^2 \tag{13}$$

where N_v is the number of skeletal units in an entanglement strand which is equal to M_e/M_v, with M_v being the molecular weight of a skeletal unit. Consequently, C_∞ also can be derived from the plateau modulus and vice versa if M_v is chosen properly:

$$C_\infty = \left(\frac{\rho RT}{3M_v G_N^0}\right)^{1/2} \tag{14}$$

Since the characteristic ratio can be derived from intrinsic viscosity[15] and the latter can be calculated from group contributions, C_∞ and M_e can also be derived from group contributions, as given by Wu:[3,16]

$$C_\infty = \left(\frac{K_\Theta}{\Phi_0}\right)^{2/3} \frac{M_v}{\langle l_v^2 \rangle} \tag{15}$$

$\Phi_0 = 2.51 \times 10^{23}$, $\langle l_v^2 \rangle$ is the average length of a skeletal unit, and K_Θ is derived from group contributions per repeat unit:

$$K_\Theta = \left(\frac{\sum_i K_i + Bn_r}{M_r}\right)^2 \tag{16}$$

where K_i are constants for groups of atoms, $B = 4.2$, and n_r is the number of skeletal atoms in the repeat unit. To calculate C_∞, we have to identify M_v and $\langle l_v^2 \rangle$ for the homopolymers and copolymers. As done by Wu, the skeletal unit of BPA-PC was chosen as half of the repeat unit, namely, from the carbonyl carbon to the isopropylidene carbon. In the case of SBI−PC the isopropylidene linkage is completely rigid, so the only logical choice is to take the whole repeat unit as the

Table 4. Scaling Parameters As Used for Wu's Model[a] (For Symbols See Text)

property	BPA-PC	SBI−PC
M_r	254.3	334.4
M_v	127.15	334.4
l_v^2	43.7	111.5
K_Θ	0.214	0.15−0.40[a]

[a] The range is due to different choices of K_i's for the phenyl rings.

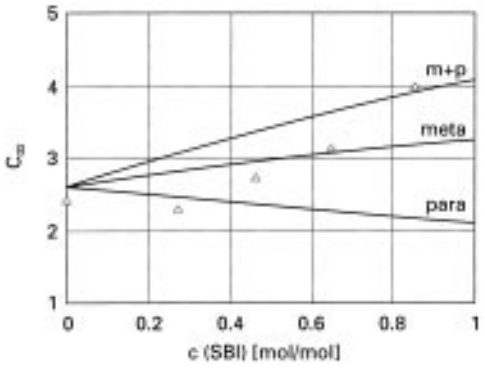

Figure 10. Characteristic ratios of copolycarbonates vs SBI content. Symbols are calculated from experiment; solid lines are the result of calculations using Wu's model for different constants of the phenyl rings. For explanation, see text.

skeletal unit. In the case of the copolymers, values were taken as the sum of weighted contributions according to their molar ratios:

$$\langle l_v^2 \rangle = \langle l_{v,1}^2 \rangle (1 - x) + \langle l_{v,2}^2 \rangle x \qquad (17)$$

where x is the molar SBI content. The value for $\langle l_v^2 \rangle$ of SBI−PC was derived from a molecular model created with Chem-X Windows.[17] The pertinent values used for the calculations are summarized in Table 4.

A main problem with the calculations is choice of the group contribution K of the phenyl rings which are linked via the spiro carbon. This contribution has not been tabulated. The ranges given in Table 4 were obtained by using the value for a para-substituted phenyl ring as the lower bound and the sum of the values for para- and meta-substituted phenyls as the upper bound in the SBI−PC. The effect of choice of that contribution is demonstrated in Figure 10, where the calculated characteristic ratios are shown as a function of the SBI content for three different cases obtained with the aid of eqs 15−17. The lower line is for para-substituted phenyls, the middle one for meta, and the top one for the sum of "para + meta" substitution. Also shown in the graph are the values derived from the experimental plateau moduli with the aid of eq 14. It will be seen that the order of magnitude has been predicted quite well. The dependence on the composition, however, has not been predicted correctly. The meta + para line fits well with the value at the highest SBI content but overpredicts at intermediate compositions. The meta line fits for intermediate compositions, and the para line fails completely at higher SBI contents. One has to keep in mind, however, that the calculated experimental points in Figure 10 are affected by the choice of M_v.

It appears that C_∞ scales more nonlinearly than predicted from group contributions. This becomes even clearer in a plot of the predicted and measured rubbery plateau moduli. A nonlinear scaling of M_e was reported for blends and statistical copolymers of PMMA.[18] For these copolymers this was ascribed to changing rotational energy barriers. This argument is reasonable for PMMA, whose chain stiffness is determined by steric hindrances in the packing of the side groups, but is not logical in the present case, where the various segments are always separated by the highly flexible carbonate units. It would be interesting to compare the present system with results of more sophisticated models as described by Bicerano[19] in order to check whether the reported deviations are due to oversimplifications inherent to the employed models.

4. Conclusions

The introduction of the SBI comonomer into BPA-PC causes all properties related to chain stiffness to change in a nonlinear fashion with composition:

(a) The glass transition temperature increases with SBI content by about 80 °C with a decreasing slope (negative curvature, opposite to the Fox relation).

(b) The entanglement molecular weight increases by more than a factor of 10 with a strong positive curvature. In terms of Tsenoglou's model this is explained by a favorable interaction between the components without leading to disentanglement.

(c) The recoverable shear compliance increases more than proportional to M_e with positive but weak curvature.

(d) The characteristic ratio determined from M_e is more than doubled.

(e) The composition dependence of the characteristic ratio is not predicted correctly by the group additivity method proposed by Wu.

Acknowledgment. The authors thank M. van Gurp of DSM, W. Zoetelief and P. Tas of Eindhoven University of Technology, and J. G. de Bruin of Philips Research for their assistance with the rheological experiments, A. J. W. Tol of Philips Research for the molecular modeling, E. S. J. Wijdenes of Philips Research for the GPC analyses, and A. Schausberger from J. Kepler University Linz and J. Wendorff from Philipps University Marburg for their helpful comments.

References and Notes

(1) Jho, J. Y.; Yee, A. F. *Macromolecules* **1991**, *24*, 1905.
(2) Sung, Y. J.; Chen, C. L.; Su, A. C. *Macromolecules* **1991**, *24*, 6123.
(3) Wu, S. *Polym. Eng. Sci.* **1992**, *32*, 823.
(4) Wu, S. *J. Appl. Polym. Sci.* **1992**, *46*, 619.
(5) Ferry, J. D. *Viscoelastic Properties of Polymers*, 3rd ed.; John Wiley & Sons: New York, 1980.
(6) Wimberger-Friedl, R. *Prog. Polym. Sci.* **1995**, *20*, 369.
(7) Stueben, K. C. *J. Polym. Sci., Part A* **1965**, *3*, 3209.
(8) Treloar, L. R. G. *Physics of Rubber Elasticity*, 3rd ed.; Oxford University Press: Oxford, U.K., 1975.
(9) Fox, T. G. *Bull. Am. Phys. Soc.* **1956**, *2*, 123.
(10) Couchman, P. R. *Polym. Eng. Sci.* **1984**, *24*, 135.
(11) Wu, S. *Polymer* **1987**, *28*, 1144; *J. Polym. Sci., Polym. Phys.* **1987**, *25*, 2511.
(12) Tsenoglou, C. *J. Polym. Sci., Polym. Phys.* **1988**, *26*, 2329.
(13) Lomellini, P.; Rossi, A. G. *Macromol. Chem.* **1990**, *191*, 1729.
(14) Schausberger, A.; Knoglinger, H.; Janeschitz-Kriegl, H. *Rheol. Acta* **1987**, *26*, 468.
(15) Flory, P. J. *Statistical Mechanics of Chain Molecules*; John Wiley & Sons: New York, 1969.
(16) Wu, S. *J. Polym. Sci., Polym. Phys.* **1989**, *27*, 723.
(17) ChemX, Chemical Design Ltd., Chipping Norton, GB. See: Davies, E. K.; Murall, N. W. *Comput. Chem.* **1989**, *13*, 149.
(18) Wu, S.; Beckerbauer, R. Paper presented at the 6th Annual Meeting of the Polymer Processing Society, Nice, France, 1990.
(19) Bicerano, J. *Prediction of Polymer Properties*; Marcel Dekker: New York, 1993.

MA951227V